Published in final edited form as:
Vet Pathol. 2008 November ; 45(6): 914–921. doi:10.1354/vp.45-6-914.

Rhesus Lymphocryptovirus Type 1-associated B-cell Nasal Lymphoma in SIV-infected Rhesus Macaques

A. K. Marr-Belvin, **A. K. Carville**, **M. A. Fahey**, **K. Boisvert**, **S. A. Klumpp**, **M. Ohashi**, **F. Wang**, **S. P. O'Neil**, and **S. V. Westmoreland**
Harvard Medical School, Department of Pathology, New England Primate Research Center, Division of Comparative Pathology, Southborough, MA (AKM, AKC, MAF, KB, SPO, SVW); The University of Texas, M. D. Anderson Cancer Center, Department of Veterinary Medicine and Surgery, Houston, TX (SAK); and Harvard Medical School, Department of Medicine, Brigham & Women's Hospital, Boston, MA (MO, FW)

Abstract

Epstein-Barr virus (EBV) is a worldwide endemic gamma herpesvirus of the genus *Lymphocryptovirus* (LCV) that infects more than 90% of the world's population. EBV has been associated with a variety of malignancies, but it has a demonstrated role in lymphomas, especially in immunosuppressed individuals. Lymphomas of the nasal cavity, paranasal sinuses, and nasopharynx are uncommon and constitute less than 5% of all extranodal lymphomas. Sinonasal non-Hodgkin's lymphomas have been reported in patients infected with human immunodeficiency virus (HIV) at an increased frequency. Rhesus LCV (rhLCV), the rhesus viral homolog of EBV, has been cloned and is associated with B-cell lymphomas in immunosuppressed rhesus macaques. We report two cases of B-cell lymphoma within the nasal cavity from 2 simian immunodeficiency virus–infected rhesus macaques with acquired immunodeficiency syndrome. The B-cell phenotype and rhLCV association were demonstrated by immunohistochemistry and confocal microscopy. The majority of the nuclei of the neoplastic B lymphocytes were EBNA-2 positive. RhLCV type 1 sequences were verified from the neoplasms by polymerase chain reaction. Nasal lymphoma is an unusual presentation of rhLCV-associated B-cell lymphoma in immunosuppressed rhesus macaques. These tumors demonstrate comparable viral pathogenesis with EBV-induced nasal lymphomas in HIV-positive people.

Keywords

EBV; lymphocryptovirus; lymphoma; macaque; rhesus; rhLCV; sinonasal; SIV

Epstein-Barr virus (EBV) is a worldwide endemic gamma herpesvirus of the genus *Lymphocryptovirus* (LCV) that infects more than 90% of the world's population, usually during childhood.[3] It is transmitted orally and persists latently in B lymphocytes generally as an asymptomatic lifelong infection. EBV has been associated with a variety of malignancies, but it has a demonstrated role in lymphomas, especially in immunosuppressed individuals. Several distinct types of EBV-associated B-cell lymphomas are known, including Hodgkin's lymphoma, Burkitt's lymphoma endemic to distinct regions of Africa with holoendemic malaria,[33] and non-Hodgkin's lymphoma (NHL) in T-cell immunocompromised patients with human immunodeficiency virus (HIV). People, especially children, living in African regions with holoendemic malaria and who have a persistent EBV-IgG antibody level, experience a

Request reprints from Susan V. Westmoreland, Harvard Medical School, Department of Pathology, New England Primate Research Center, One Pine Hill Drive, Southborough, MA 01772-9102 (USA). E-mail: susan_westmoreland@hms.harvard.edu.

30-fold increased risk of developing Burkitt's lymphoma affecting the facial and abdominal lymph nodes. In addition, persons undergoing iatrogenic immunosuppression for organ transplantation are also noted to have a higher incidence of EBV-associated post-transplant lymphoproliferative disorders as well as lymphomas, and almost all of the tumors arise within the first year of allografting are EBV-positive.[33]

The simian immunodeficiency virus (SIV)–infected rhesus macaque (*Macaca mulatta*) is a well-established model of acquired immunodeficiency syndrome (AIDS) sharing similarities with HIV-infected people in disease course and progression, immunologic response, and the spectrum of opportunistic infections.[17] In particular, EBV, an important opportunistic infection in patients with AIDS, has homologous LCVs that naturally infect Old World and New World primates.[22,23] In the SIV-infected rhesus, LCV causes lytic epithelial infection[18] and lymphoma[15] similar to that seen in people with AIDS. Like EBV, there are 2 distinct variants of rhesus LCV (rhLCV), types 1 and 2.[10] The complete RhLCV genome was recently sequenced and was found to have an identical repertoire of lytic and latent infection genes as EBV.[23–25] In addition, latent infection of rhLCV has been linked to the development of lymphomas in SIV-infected rhesus macaques at an incidence of 4%, similar to that seen in HIV-infected individuals.[11,15] An excellent recent review of the pathobiology of macaque LCVs has been published by Carville and Mansfield.[8] Only a few mentions of nasal cavity lymphoma have been reported in macaques. A review of lymphomas in 16 SIV-infected rhesus monkeys with AIDS from the German Primate Center, Gottingen, Germany, presented 14 of 16 monkeys with CD20 immunopositive B-cell lymphomas in multiple sites, including the nasal cavity, but the report did not characterize the nasal lymphomas further.[15] Recently, a case of spontaneous NK/T cell lymphoma present in the nasal cavity in addition to lymphoid and visceral tissues was reported in a Japanese macaque.[28] Here we present two cases of rhLCV type 1 associated nasal B-cell lymphomas in SIV-immunosuppressed rhesus macaques, demonstrating parallel viral pathogenesis with EBV-induced nasal lymphomas in HIV-positive people with AIDS.

Materials and Methods

Two rhesus macaques (Mm 95-00, macaque No. 1, and Mm 289-98, macaque No. 2, Table 1) were studied. A 2-year-old male rhesus macaque (macaque No. 1) was acquired from the Caribbean Primate Research Center by the New England Primate Research Center (NEPRC). On arrival, he was quarantined for 45 days, during which time he was screened for simian retroviruses (SRV-D, STLV, and SIV) and Herpes simiae (B virus) by serology; *Salmonella*, *Campylobacter*, and enteropathogenic *Escherichia coli* by fecal culture; and tuberculosis by intradermal testing. In addition, he was vaccinated for measles and treated with ivermectin for parasites. Three years later he was inoculated intravenously with SIVmac239. Two years after inoculation, a mass was noted in the right nostril with progressive facial swelling, and the animal was euthanized for diagnostic necropsy. The second rhesus macaque (macaque No. 2) was born at NEPRC and was group-housed in the conventional colony with biannual health checks until assigned to a study at age 7. He was moved to individual housing before intravenous inoculation with SIVmac251 and CD4-depleted with anti-CD4 antibody using a previously described depletion protocol. [22] A year and a half after inoculation he developed signs of weight loss and upper respiratory disease and was euthanized for diagnostic necropsy.

At the time of necropsy, representative tissues from all major organ systems were collected, fixed in 10% neutral-buffered formalin, embedded in paraffin blocks, sectioned at 5 μm, and stained with hematoxylin and eosin by routine techniques. Additional sections were used for immunohistochemistry and immunofluorescence. Additional pieces of tissue were collected

and frozen in microcentrifuge tubes on dry ice and stored at −80°C for polymerase chain reaction (PCR).

To immunophenotype the neoplastic cell population in both tumors, we used standard immunoperoxidase staining for T cells (CD3), B cells (CD20), and natural killer (NK) T cells (CD56, NCAM) using standard avidin-biotin-peroxidase (ABC) complex technique (Dako, Carpinteria, CA). We also evaluated EBV-encoded nuclear antigen (EBNA-2), Bcl-2, Ki-67, topoisomerase II, and p53. Briefly, formalin-fixed paraffin-embedded 5-µm sections were deparaffinized and rehydrated followed by H_2O_2 block of endogenos peroxidase, microwave antigen retrieval, and Dako protein block. Sections were incubated with rabbit anti-human CD3 (Dako, polyclonal, 1 : 600, 30′, RT), mouse anti-human CD20 (Dako, L26, IgG2a : 175, overnight, 4°C), mouse anti-human CD56 (Zymed, San Francisco, CA, N-CAM, IgG1, 1 : 500, overnight, 4°C), mouse anti-human EBNA-2 (Dako, PE2, IgG1, 1 : 5,200, overnight, 4°C), mouse anti-human Bcl-2 (Dako, 124. IgG1 1 : 110, 60′, RT), mouse anti-human Ki-67 antigen (Dako, MIB-1, IgG1, 1 : 80, 60′, RT), mouse anti-human topoisomerase II alpha (Dako, SWT3D1, IgG1, 1 : 75, 60′, RT), or mouse anti-human p53 (Dako, DO-7, IgG2b, 1 : 390, 30′, RT). Slides were then incubated with the secondary antibody (biotinylated goat anti-rabbit [Vector Laboratories, Burlingame, CA, IgG, 1 : 200, 30′, RT] for CD3 and biotinylated horse anti-mouse [Vector Laboratories, IgG, 1 : 200, 30′, RT] for CD20, CD56, EBNA-2, Bcl-2, Ki-67, topoisomerase II alpha, and p53) followed by a 30-minute incubation with Vectastain ABC Elite, except CD20 incubated with ABC standard. Tissue sections were washed and developed with DAB chromagen (Dako) and counter-stained with Mayer's hematoxylin. Step sections were incubated with isotype-specific irrelevant antibodies for negative controls.

EBV nuclear antigen, EBNA-2, is an EBV protein expressed in latent infection. The expression of EBNA-2 was evaluated using a monoclonal antibody that is known to cross-react in rhesus with a conserved epitope in the carboxy-terminal transactivating domain.[17,22] The coexpression of LCV Epstein-Barr nuclear antigen-2 (EBNA-2) protein in the neoplastic B cells was examined by double-label immunofluorescence with anti-EBNA-2 and anti-CD20 by laser confocal microscopy. Briefly, 5-µm thick sections of formalin-fixed paraffin-embedded tissue were deparaffinized, rehydrated, and washed in 1× phosphate-buffered saline (PBS) containing 0.2% fish skin gelatin (FSG) (1×PBS/FSG). Sections were heated in antigen unmasking solution (Dako) for antigen retrieval. Sections were blocked with 10% normal goat serum (diluted with 1 × PBS/FSG) for 20 minutes followed by Dako-Biotin Blocking system solutions, then incubated with anti-EBNA-2 antibody (Dako, PE2, IgG1, 1 : 520) and anti-CD20 antibody (Dako, L26, IgG2b, 1 : 18) for 1 hr RT. Biotinylated goat anti-mouse IgG_1 antibody (Vector Labs, 1 : 200 dilution) was applied to the slide for 30 minutes, followed by streptavidin conjugated with Alexa 488 (green) (Molecular Probes, Eugene, OR, 1 : 1,000) for 30 minutes to detect EBNA-2 followed by secondary goat anti-mouse directly conjugated with Alexa 568 (red) (Molecular Probes, 1 : 1,000) for 30 minutes to detect CD20 positive B cells. Slides were treated with nuclear stain Topro-3 1 : 5,000 for 5 minutes RT, then washed and coverslipped. Serial sections were incubated with isotype-matched negative control antibodies.

Laser confocal microscopy was performed using a Leica TCS SP laser-scanning microscope equipped with 3 lasers (Leica Microsystems, Exton, PA). The fluorescence of individual fluorochromes are captured simultaneously, after optimization to reduce bleed through between channels (photomultiplier tubes), using the Leica software. Images were collected at 512×512 pixel resolution.

To test for the presence and type of rhLCV in the tumors, DNA was extracted using DNeasy kits (Qiagen, Valencia, CA) followed by PCR amplification of sequences of macaque homologues to EBV. Amplification was performed using primers for herpesvirus *Macaca fascicularis* 1 (HVMF-1) W/IR1 region (299 bp)[14] (Invitrogen, Carlsbad, CA) and rhLCV

EBER gene (117 bp)[23] (Invitrogen, Carlsbad, CA). We used β-actin (306 bp) (Genebank AK223055.1 and M10277 gene) to confirm that samples contained amplifiable DNA. PCR amplification was done as described previously[14,23] using GoTaq Green Master Mix (Promega, Madison, WI) and 100–150 ng of DNA. PCR products were visualized on 2% agarose gel (SeaKem LE Agarose, Cambrex, Rock-land, ME) containing 100 pg/μl ethidium bromide (Sigma, St. Louis, MO).

The rhLCV type-specific PCR was performed as previously described.[10] In brief, type 1 rhLCV EBNA-2 (that is, sequence derived from LCL8664) specific primers T1E2F (5′-TAAAGTTCCAACTGTGCAAT-3′) and T1E2R (5′-CTTTGCCCTTGCCCTTTTG-3′) and type 2 rhLCV EBNA-2 (that is, sequence derived from 208-95 tumor) specific primers T2E2F (5′-TGCCCCAAGAGTAGTAACA-3′) and T2E2R (5′-TTAGGACGGCCTGGTGGAC-3′) were used with the following cycling conditions: 95°C for 5 minutes and 40 cycles of denaturing at 95°C for 30 seconds, annealing 60°C for 30 seconds, and extending 72°C for 30 seconds. PCR products were visualized by ultraviolet illumination after gel electrophoresis with ethidium bromide staining.

Results

Clinical history and gross findings

Macaque No. 1 had been inoculated intravenously with SIVmac239 approximately 26 months before euthanasia. A mass was noted in the right nostril with progressive facial swelling the day before euthanasia. Postmortem examination revealed marked swelling of the right side of the face with swollen eyelids and mild swelling of the left side of the face. A small amount of purulent material was present at the medial canthus of the right eye and the right nostril. An off-white mass partially occluded the right nasal lumen and infiltrated the soft palate. The nasal cavity was hemisectioned for histologic examination (Fig. 1). The remainder of the necropsy findings included good physical condition, moderately enlarged spleen, and peripheral lymph nodes with prominent submandibular and cervical lymph nodes. Generalized lymphadenopathy is consistent with SIV infection.

Macaque No. 2 was inoculated with SIVmac251 and CD4-depleted with anti-CD4 antibody (protocol previously described[22]) approximately 18 months before euthanasia at which time he exhibited signs of weight loss and upper respiratory disease. The macaque was well muscled but had decreased body fat. Gross examination revealed a mass of mucopurulent debris in the left the nasal cavity, generalized lymphadenopathy, and incompletely deflated, slightly firm lung.

Histopathologic findings

Histopathologic examination of the nasopharynx of macaque No. 1 and the sinonasal cavity of macaque No. 2 revealed very similar expansile and unencapsulated neoplasms that distorted and effaced the nasal turbinates and were composed of densely cellular sheets of round cells separated by fine fibrovascular stroma consistent with lymphoma (Fig. 2). The round cells of both neoplasms were composed of a population of centroblasts with 8–10 μm round to oval and occasionally indented centrally placed nuclei with euchromatin and prominent single nucleoli, variably indistinct cell margins and moderate amounts of eosinophilic homogenous cytoplasm admixed with infiltrating and residual small mature lymphocytes (Fig. 3). Both neoplasms had increased mitotic rate of 2 to 4 mitotic figures per high power field. The nasal lymphoma in the first macaque had resulted in osteolysis and partial destruction of bones of the nasal septum and multifocal abscesses with intralesional mixed population of bacteria. There were multifocal areas of extensive necrosis, hemorrhage, and macrophages laden with

golden-brown pigment (hemosiderin). Multifocal areas of mucosal acanthosis and submucosal fibrosis were present and concentrated perivascularly.

Other histologic findings for macaque No. 1 included submandibular salivary gland herpesviral cytomegalovirus (CMV), an AIDS-defining lesion associated with immunosuppression, and lymph node follicular hyperplasia, consistent with SIV. Other histologic findings in macaque No. 2 included generalized follicular hyperplasia of the lymph nodes and expansion of the periarteriolar lymphoid sheaths consistent with SIV, as well as multifocal, necrotizing severe aspiration bronchopneumonia.

Lymphomas are CD20 and EBNA-2 positive with increased proliferation and decreased apoptosis

Immunohistochemical analysis of cellular constituents was similar in both cases of nasal lymphoma. The majority of cells were neoplastic B lymphocytes exhibiting diffuse cell membrane reactivity with anti-CD20 (Fig. 4). In addition, most of the cells expressed nuclear reactivity with anti-EBNA-2 (Fig. 11). There were occasional cells with diffuse anti-CD3 cytoplasmic reactivity (Fig. 5) and rare cells with diffuse anti-CD56 cell membrane reactivity (Fig. 6) indicating T lymphocyte and NK cell infiltrates, respectively. Based on these observations, both masses were diagnosed as B-cell lymphomas. In addition, 5%–10% of the cells exhibited nuclear immunoreactivity to the anti-apoptotic protein Bcl-2 (Fig. 7), while most of the cells expressed the nuclear proliferation antigen Ki-67 (Fig. 8), found in cells in the active phases of the cell cycle, and topoisomerase II (Fig. 9), a marker of cellular proliferation, consistent with rapidly proliferating tumor cells. Aberrant nuclear expression of tumor suppressor p53 was demonstrated in 30%–60% of the neoplastic cells (Fig. 10).

Neoplastic CD20-positive B cells coexpress nuclear EBNA-2 protein

We verified the presence of rhLCV EBNA-2 protein in the neoplastic B lymphocytes using double-label immunofluorescence and laser confocal microscopy. The majority of the neoplastic cells were CD20-positive B lymphocytes (red) exhibiting EBNA-2 protein in the nucleus (green) (Fig. 12).

Macaque lymphocryptovirus amplified from nasal lymphomas

We confirmed that rhLCV was present in both nasal lymphomas. Gene products of the amplified sequences of the HVMF-1 W/IR1 region and the rhLCV EBER gene were detected at appropriate sizes, 299 bp and 117 bp, respectively (data not shown). Water controls were negative. Gene products of the amplified sequences of type 1 EBNA-2 were also detected for both macaques (Fig. 13).

Discussion

We report 2 cases of nasal lymphoma in SIV-infected immunocompromised rhesus macaques that are large B-cell lymphomas associated with rhesus LCV type 1. Tumor cells harbor rhLCV type 1 viral DNA and express the latent viral protein EBNA-2. Both lymphoma cases also exhibited increased antiapoptotic expression of Bcl-2, increased Ki-67 and topoisomerase activity, and aberrant expression of tumor suppressor gene p53. These tumors are comparable to those seen in HIV-infected patients with AIDS with a similar viral pathogenesis involving a homologue to EBV, rhLCV.

Lymphomas of the nasal cavity, paranasal sinuses, and nasopharynx are uncommon and constitute less than 5% of all extranodal lymphomas in people.[11,30] Geographic distribution typically corresponds to cell-type variation of lymphomas in these anatomic sites. In Western countries, nasal-type lymphomas are typically diffuse large B-cell lymphomas arising in

elderly patients within the paranasal sinuses,[30] whereas in Eastern countries and South America T-cell or natural killer cell lymphomas are more common in younger patients and within the nasal cavity.[1,9,19,30] Both types of nasal lymphomas have been associated with EBV.[11]

The pathogenesis of opportunistic infections secondary to immunosuppression caused by HIV is currently being researched. Decreased CD4 counts have been associated with increased opportunistic infection;[27] however, they are not sufficient for the induction of LCV-induced lymphomas.[23] Likewise, rhLCV alone may not be sufficient for malignant conversion of latently infected cells.[23] A very recent publication shows that HIV patients developing primary central nervous system lymphoma lack EBV-specific CD4+ T-cell function irrespective of absolute CD4+ T-cell counts,[12] which supports a synergistic pathogenesis of lymphoma in immunosuppressed patients.

Recently, excellent reviews of the latency and reactivation of EBV have been written.[2,7,29,32] In summary, EBV is transmitted by close contact with viral infection beginning in the nasopharyngeal and oropharyngeal lymphoid tissues, and EBV establishes a lifelong latent infection in a small population of B cells. EBNA-2 is the first viral protein expressed in infection of primary B lymphocytes and is essential for EBV-mediated cell growth and transformation through transcriptional activation. EBNA-2 activates specific viral and cellular promoters, including the LMP1 promoter.

In addition, high Ki-67, Bcl2, p53, and topoisomerase expression have been shown to correlate with high-grade B-cell lymphomas and rapid disease progression.[4,31] Genomic instability with chromosomal translocations and somatic mutations have been hypothesized as the second step in EBV-associated oncogenesis.[6,20] This may be directly influenced by EBV's ability to persistently infect B cells and its ability to induce genomic instability by enhancing recombinase activity.[26]

In addition to immunosuppression and genomic instability, proposed factors involved in the development of lymphoma include chronic inflammation. The preponderance of lymphoma within the gastro-intestinal tract of multiple species and sinonasal cavities supports this theory. Patients with AIDS have high levels of proinflammatory cytokines, some of which are growth factors for B cells, which likely play a role in AIDS-associated B-cell neoplasms.[16] NF-κB cellular induction has been proposed as a central molecular step in carcinogenesis.[5,13,16,21]

In conclusion, the 2 rhesus macaques described in this report were diagnosed with rhLCV-associated B-cell type nasal lymphoma as indicated by positive rhLCV type 1 EBER gene PCR and immunoreactivity with CD20 and EBNA-2 with a subpopulation ofCD3+ T cells and rare CD56+NK cells infiltrating the neoplasm. Based on these data, nasal cavity lymphoma in SIV-infected rhesus macaques has a common etiology and pathogenesis to EBV-associated nasal cavity lymphomas seen in AIDS patients.

Acknowledgements

We thank Kristen Toohey for graphic services and Douglas Pauley for technical services. This research was funded in part by grants RR00168 and RR07000.

The animals described in this article were housed and treated in accordance with standards of the Association for Assessment and Accreditation of Laboratory Animal Care and Harvard Medical School's Animal Care and Use Committee.

References

1. Abbondanzo SL, Wenig BM. Non-Hodgkin's lymphoma of the sinonasal tract. A clinicopathologic and immunophenotypic study of 120 cases. Cancer 1995;75:1281–1291. [PubMed: 7882278]

2. Amon W, Farrell PJ. Reactivation of Epstein-Barr virus from latency. Rev Med Virol 2005;15:149–156. [PubMed: 15546128]
3. Andersson J. Epstein-Barr virus and Hodgkin's lymphoma. Herpes 2006;13:12–16. [PubMed: 16732997]
4. Bai M, Tsanou E, Skyrlas A, Sainis I, Agnantis N, Kanavaros P. Alterations of the p53, Rb and p27 tumor suppressor pathways in diffuse large B-cell lymphomas. Anticancer Res 2007;27:2345–2352. [PubMed: 17695524]
5. Balkwill F, Coussens LM. Cancer: an inflammatory link. Nature 2004;431:405–406. [PubMed: 15385993]
6. Ballerini P, Gaidano G, Gong JZ, Tassi V, Saglio G, Knowles DM, Dalla-Favera R. Multiple genetic lesions in acquired immunodeficiency syndrome-related non-Hodgkin's lymphoma. Blood 1993;81:166–176. [PubMed: 8380252]
7. Bornkamm GW, Hammerschmidt W. Molecular virology of Epstein-Barr virus. Philos Trans R Soc Lond B Biol Sci 2001;356:437–459. [PubMed: 11313004]
8. Carville A, Mansfeld KG. Comparative pathobiology of macaque lymphocryptoviruses. Comp Med 2008;58:52–62.
9. Cheung MM, Chan JK, Lau WH, Foo W, Chan PT, Ng CS, Ngan RK. Primary non-Hodgkin's lymphoma of the nose and nasopharynx: clinical features, tumor immunophenotype, and treatment outcome in 113 patients. J Clin Oncol 1998;16:70–77. [PubMed: 9440725]
10. Cho YG, Gordadze AV, Ling PD, Wang F. Evolution of two types of rhesus lymphocryptovirus similar to type 1 and type 2 Epstein-Barr virus. J Virol 1999;73:9206–9212. [PubMed: 10516028]
11. Cleary KR, Batsakis JG. Sinonasal lymphomas. Ann Otol Rhinol Laryngol 1994;103:911–914. [PubMed: 7979008]
12. Gasser O, Bihl FK, Wolbers M, Loggi E, Steffen I, Hirsch HH, Gunthard HF, Walker BD, Brander C, Battegay M, Hess C. HIV patients developing primary CNS lymphoma lack EBV-specific CD4 + T cell function irrespective of absolute CD4+ T cell counts. PLoS Med 2007;4:e96. [PubMed: 17388662]
13. Greten FR, Eckmann L, Greten TF, Park JM, Li ZW, Egan LJ, Kagnoff MF, Karin M. IKKbeta links inflammation and tumorigenesis in a mouse model of colitis-associated cancer. Cell 2004;118:285–296. [PubMed: 15294155]
14. Habis A, Baskin G, Simpson L, Fortgang I, Murphey-Corb M, Levy LS. Rhesus lymphocrypto-virus infection during the progression of SAIDS and SAIDS-associated lymphoma in the rhesus macaque. AIDS Res Hum Retroviruses 2000;16:163–171. [PubMed: 10659055]
15. Kahnt K, Matz-Rensing K, Hofmann P, Stahl-Hennig C, Kaup FJ. SIV-associated lymphomas in rhesus monkeys (*Macaca mulatta*) in comparison with HIV-associated lymphomas. Vet Pathol 2002;39:42–55. [PubMed: 12102218]
16. Khan G. Epstein-Barr virus, cytokines, and inflammation: a cocktail for the pathogenesis of Hodgkin's lymphoma? Exp Hematol 2006;34:399–406. [PubMed: 16569586]
17. King NW, Chalifoux LV, Ringler DJ, Wyand MS, Sehgal PK, Daniel MD, Letvin NL, Desrosiers RC, Blake BJ, Hunt RD. Comparative biology of natural and experimental SIVmac infection in macaque monkeys: a review. J Med Primatol 1990;19:109–118. [PubMed: 2160016]
18. Kutok JL, Klumpp S, Simon M, MacKey JJ, Nguyen V, Middeldorp JM, Aster JC, Wang F. Molecular evidence for rhesus lymphocryptovirus infection of epithelial cells in immunosuppressed rhesus macaques. J Virol 2004;78:3455–3461. [PubMed: 15016868]
19. Logsdon MD, Ha CS, Kavadi VS, Cabanillas F, Hess MA, Cox JD. Lymphoma of the nasal cavity and paranasal sinuses: improved outcome and altered prognostic factors with combined modality therapy. Cancer 1997;80:477–488. [PubMed: 9241082]
20. Pasqualucci L, Neumeister P, Goossens T, Nanjangud G, Chaganti RS, Kuppers R, Dalla-Favera R. Hypermutation of multiple proto-oncogenes in B-cell diffuse large-cell lymphomas. Nature 2001;412:341–346. [PubMed: 11460166]
21. Pikarsky E, Porat RM, Stein I, Abramovitch R, Amit S, Kasem S, Gutkovich-Pyest E, Urieli-Shoval S, Galun E, Ben-Neriah Y. NF-kappa B functions as a tumour promoter in inflammation-associated cancer. Nature 2004;431:461–466. [PubMed: 15329734]

22. Reimann KA, Lin W, Bixler S, Browning B, Ehrenfels BN, Lucci J, Miatkowski K, Olson D, Parish TH, Rosa MD, Oleson FB, Hsu YM, Padlan EA, Letvin NL, Burkly LC. A humanized form of a CD4-specific monoclonal antibody exhibits decreased antigenicity and prolonged plasma half-life in rhesus monkeys while retaining its unique biological and antiviral properties. AIDS Res Hum Retroviruses 1997;13:933–943. [PubMed: 9223409]

23. Rivailler P, Carville A, Kaur A, Rao P, Quink C, Kutok JL, Westmoreland S, Klumpp S, Simon M, Aster JC, Wang F. Experimental rhesus lymphocryptovirus infection in immunosuppressed macaques: an animal model for Epstein-Barr virus pathogenesis in the immunosuppressed host. Blood 2004;104:1482–1489. [PubMed: 15150077]

24. Rivailler P, Cho YG, Wang F. Complete genomic sequence of an Epstein-Barr virus-related herpesvirus naturally infecting a new world primate: a defining point in the evolution of oncogenic lymphocryptoviruses. J Virol 2002;76:12055–12068. [PubMed: 12414947]

25. Rivailler P, Jiang H, Cho YG, Quink C, Wang F. Complete nucleotide sequence of the rhesus lymphocryptovirus: genetic validation for an Epstein-Barr virus animal model. J Virol 2002;76:421–426. [PubMed: 11739708]

26. Srinivas SK, Sixbey JW. Epstein-Barr virus induction of recombinase-activating genes RAG1 and RAG2. J Virol 1995;69:8155–8158. [PubMed: 7494341]

27. Stein DS, Korvick JA, Vermund SH. CD4+ lymphocyte cell enumeration for prediction of clinical course of human immunodeficiency virus disease: a review. J Infect Dis 1992;165:352–363. [PubMed: 1346152]

28. Suzuki J, Goto S, Kato A, Hashimoto C, Miwa N, Takao S, Ishida T, Fukuoka A, Nakayama H, Doi K, Isowa K. Malignant NK/T-cell lymphoma associated with simian Epstein-Barr virus infection in a Japanese macaque (*Macaca fuscata*). Exp Anim 2005;54:101–105. [PubMed: 15725687]

29. Tsurumi T, Fujita M, Kudoh A. Latent and lytic Epstein-Barr virus replication strategies. Rev Med Virol 2005;15:3–15. [PubMed: 15386591]

30. Vega F, Lin P, Medeiros LJ. Extranodal lymphomas of the head and neck. Ann Diagn Pathol 2005;9:340–350. [PubMed: 16308165]

31. Yamanaka N, Harabuchi Y, Kataura A. The prognostic value of Ki-67 antigen in non-Hodgkin lymphoma of Waldeyer ring and the nasal cavity. Cancer 1992;70:2342–2349. [PubMed: 1394063]

32. Young LS, Murray PG. Epstein-Barr virus and oncogenesis: from latent genes to tumours. Oncogene 2003;22:5108–5121. [PubMed: 12910248]

33. Young LS, Rickinson AB. Epstein-Barr virus: 40 years on. Nat Rev Cancer 2004;4:757–768. [PubMed: 15510157]

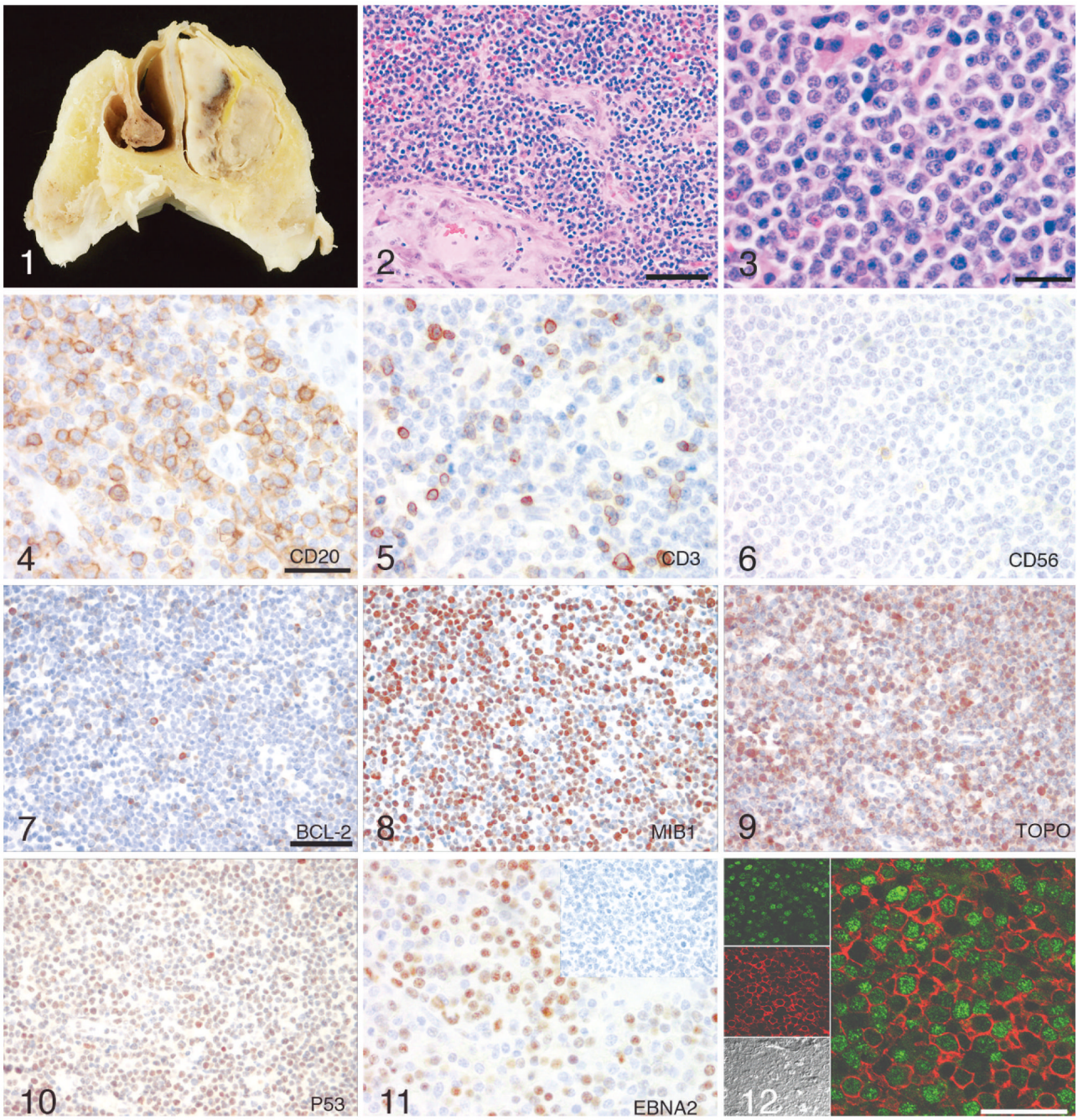

Fig. 1. Nasal cavity; macaque No. 1. A gray-green mass partially occluded the lumen of the right nostril with an off-white mass posterior to and contiguous with the gray-green mass.
Fig. 2. Nasal lymphoma; macaque No. 2. Neoplasm composed of densely cellular sheets of round cells which effaces and replaces the turbinates and extends to tissue section margins. HE. Bar = 80 μm.
Fig. 3. B-cell lymphoma, higher magnification; macaque No. 2. HE. Bar = 40 μm.
Fig. 4. B-cell lymphoma; macaque No. 2. The majority of cells demonstrate diffuse cell membrane reactivity with anti-CD20 indicating B lymphocytes. Immunoperoxidase staining, DAB chromagen, Mayer's hematoxylin counterstain. Bar = 40 μm.

Fig. 5. B-cell lymphoma; macaque No. 2. Occasional cells have diffuse anti-CD3 cytoplasmic reactivity indicating T lymphocytes. Immunoperoxidase staining, DAB chromagen, Mayer's hematoxylin counterstain. Bar = 40 μm.

Fig. 6. B-cell lymphoma; macaque No. 2. Occasional cells have diffuse anti-CD56 cell membrane reactivity indicating NK cells. Immunoperoxidase staining, DAB chromagen, Mayer's hematoxylin counterstain. Bar = 20 μm.

Fig. 7. B-cell lymphoma; macaque No. 2. Approximately, 20% of the B lymphocytes have cytoplasmic reactivity with anti-Bcl-2. Immunoperoxidase staining, DAB chromagen, Mayer's hematoxylin counterstain. Bar = 40 μm.

Fig. 8. B-cell lymphoma; macaque No. 2. Approximately, 80% of the B lymphocytes have cytoplasmic and nuclear reactivity with anti-MIB1. Immunoperoxidase staining, DAB chromagen, Mayer's hematoxylin counterstain. Bar = 40 μm.

Fig. 9. The majority of the B lymphocytes have cytoplasmic reactivity with anti-topoisomerase II alpha. Immunoperoxidase staining, DAB chromagen, Mayer's hematoxylin counterstain. Bar = 40 μm.

Fig. 10. Approximately, 30%–60% of the B lymphocytes have nuclear reactivity with anti-p53. Immunoperoxidase staining, DAB chromagen, Mayer's hematoxylin counterstain. Bar = 40 μm.

Fig. 11. B-cell lymphoma; macaque No. 2. Frequent B lymphocytes exhibit nuclear immunoreactivity with anti-EBNA-2; inset: nonlymphomatous lymph node from the same animal exhibits no reactivity with EBNA-2. Immunoperoxidase staining, DAB chromagen, Mayer's hematoxylin counterstain. Bar = 40 μm.

Fig. 12. B-cell lymphoma; macaque No. 2. Immunofluorescence anti-CD20 cytoplasmic (red) and anti-EBNA2 nuclear (green) colocalization demonstrating EBNA2 positive B-cell nasal lymphoma. Confocal.

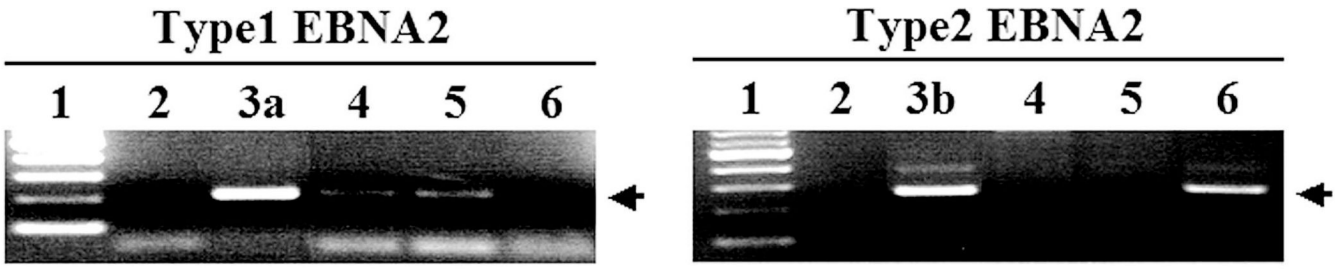

13

Fig. 13.

PCR amplifications for type 1 and type 2 rhLCV EBNA-2 were performed with genomic DNA extracted from macaque No. 1 (lane 4) and macaque No. 2 (lane 5) tissue sections and the 208-95 tumor cell line known to be infected with type 2 rhLCV (lane 6). PCR amplifications with no template DNA (lane 2), genomic DNA from type 1 rhLCV-infected cells (lane 3a) or type 2 rhLCV EBNA2 plasmid DNA (lane 3b) are shown as controls. One hundred base pair molecular weight markers are shown in lane 1, and migration of the 212 bp type 1 rhLCV EBNA-2 or 260 bp type 2 rhLCV EBNA-2 is indicated by the arrows.

Table 1

Case summaries.

Animal No.	Sex	Age at Death	Inoculum	Survival*	Gross Findings
Case No. 1	M	7 years	SIVmac239 IV	774 days	Mass in right nostril with facial swelling
Case No. 2	M	7 years	SIVmac251 IV and CD4 depletion	540 days	Mass of mucopurulent debris removed from nasal cavity; generalized lymphadenopathy

* Survival days after inoculation with virus.

Table 2

Immunohistochemistry.*

Animal #	CD20	CD3	CD56	EBNA-2	Bcl-2	P53	Topoisomerase	Ki-67
Case No. 1	+	−	−	+	ND	++	++	++
Case No. 2	+++	+	(+)	+++	+	+++	+++	+++

*ND = not done; − = no staining; (+) = 5% to <10% + = 10% to <30% ++ = 30% to <60% +++ = 60% to 100%.